ChemComm

COMMUNICATION

Cite this: *Chem. Commun.*, 2018, **54**, 771

Received 26th November 2017,
Accepted 27th December 2017

DOI: 10.1039/c7cc09086b

rsc.li/chemcomm

Scission and stitching of adenine structures by water molecules†

Chi Zhang, Lei Xie, Yuanqi Ding and Wei Xu *

Based on high-resolution STM imaging/manipulations and DFT calculations, we display the dynamic hydration process of adenine networks on Au(111) in real space, which results in controllable scission and stitching of adenine structures by water molecules.

Water, with many oddities in its physical and chemical made-up, plays a pervasive and also unique role in nature.[1] Various physico-chemical phenomena with the participation of water (*e.g.* the adsorption and dynamics of water adsorbed on solid surfaces) are vital for many scientific and technological areas such as catalysis, electrochemistry, and corrosion.[1–3] Pioneering studies demonstrated the versatility of scanning tunneling microscopy (STM) under ultra-high vacuum (UHV) conditions and theoretical calculations in investigating water on surfaces. By virtue of both experimental and theoretical evidence, the structures of water clusters[3–8] and overlayers,[9–14] and also dynamic behaviors of water such as diffusion and clustering on surfaces,[5,15] have been extensively explored.[2] Recently, the interactions between water and organic molecules on surfaces were studied, in which water is found to play a vital role in determining the molecular conformation of a single molecule,[16] influencing the supramolecular network of azobenzene molecules,[17] and also inducing the tautomerization of guanine molecules.[18] However, detailed explorations of dynamic hydration of organic molecules on surfaces, to the best of our knowledge, has not been reported hitherto. It is thus intriguing to explore the interactions between water and organic molecules and further unravel the water-induced dynamic process of organic molecules on the surfaces, which may shed light on the fundamental understanding of the interactions between water and organic molecules on the atomic scale.

As revealed from previous theoretical studies,[19,20] the canonical form of an adenine (A) molecule is the global minimum in the gas phase, in a microhydrated environment and also in the bulk water. It has also been well established that DNA molecules are hydrated *in vivo* and derive their structures, functions, and activities from their interactions with water molecules.[21] We thus choose adenine as the potential candidate to investigate the interaction between water and adenine molecules. From the interplay of high-resolution STM imaging/manipulations and density functional theory (DFT) calculations, we display the dynamic hydration process of adenine molecular networks on Au(111) in real space, which results in controllable scission and stitching of adenine structures by water molecules. Dosing water on the A-island-precovered Au(111) surface held at room temperature (RT) in a controlled stepwise manner results in the breakage of A islands by perturbing the weakest hydrogen bonding sites and the simultaneous formation of single adenine rows in the first step (*i.e.*, water-induced scission process), and then a larger amount of water leads to the gradual growth of A-H_2O islands which are composed of such adenine rows bridged by water molecules *via* hydrogen bonds (*i.e.*, water-induced stitching process). Interestingly, reversible formation and breakage of such A-H_2O islands is achieved as water molecules in the islands can be removed *via* thermal treatment and re-adsorb by further dosing. Moreover, lateral STM manipulations enable us to remove or move water molecules in the islands, thus presenting dynamics of the hydration process. These findings provide the real-space determination of interactions between water and organic molecules adsorbed on a surface. Such results may also provide implications for biological processes and heterogeneous catalyses which are strongly dependent on or even driven by solvent effects.

After deposition of adenine molecules on Au(111) held at RT at ~0.5 monolayer (ML), ordered A islands are formed (Fig. 1a) as reported.[22,23] Subsequent exposure of the A-precovered sample (held at RT) to the water atmosphere at a pressure of $\sim 1 \times 10^{-6}$ mbar for 10 min surprisingly leads to the disassembly of the A islands and simultaneous formation of molecular rows (Fig. 1b). It can also be seen that each row is made up of characteristic six-membered rings of A molecules (detailed in Fig. S1, ESI†), and the blurs around the rows show their mobility and trajectories. Along the edges of the rows, the water molecules may also diffuse[8] (typically indicated by the white arrow in Fig. 1b). It is important to emphasize that even at ~4.8 K, water molecules

---

Interdisciplinary Materials Research Center, College of Materials Science and Engineering, Tongji University, Shanghai 201804, P. R. China. E-mail: xuwei@tongji.edu.cn

† Electronic supplementary information (ESI) available: Experimental details, supplementary STM images and line profiles. See DOI: 10.1039/c7cc09086b

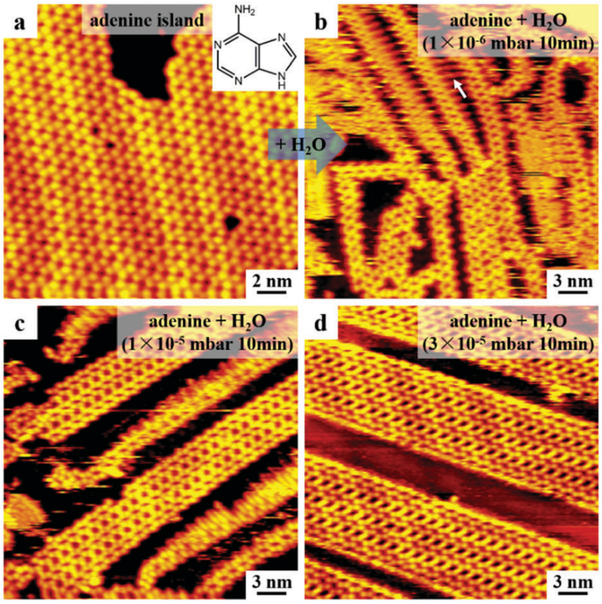

Fig. 1 Scission and stitching processes of adenine islands by gradually increasing water dosages on Au(111). (a) STM image showing the formation of ordered adenine islands (~0.5 ML) after deposition of adenine molecules on Au(111) held at RT. (b) STM image showing the appearance of single adenine molecular rows after exposing the A-precovered surface (held at RT) to the water atmosphere at a pressure of ~1 × 10^{-6} mbar for 10 min. (c) STM image showing the growth of small patches of rectangular islands after exposing the above sample (at RT) to the water atmosphere at a pressure of ~1 × 10^{-5} mbar for 10 min. (d) STM image showing the formation of larger rectangular islands by further increasing the water dosage at a pressure of ~3 × 10^{-5} mbar for 10 min. Scanning conditions: I_t = 0.7 nA, V_t = −1.5 V.

were still able to walk along the edges of a pentagonal water chain on Cu(110) (with the formation and breakage of OH···O hydrogen bonds) as reported,[8] indicating the difficulty in trapping single water molecules at the edges. Besides, it is also reported[5] that after the deposition of water molecules (D_2O) on the cooled Au(111) (25 K), water monomers or larger clusters can adsorb at the elbow sites of the herringbone reconstruction, where STM imaging was performed at 5.5 K. However, water molecules are so weakly bound on Au(111) that they can be easily moved even at the elbow sites during scanning. What's more, a combined experimental and theoretical study[24] has demonstrated that the Au(111) surface is hydrophobic and the interaction between the water molecules and the surface is very weak. In the most recent paper,[25] Au(111) is also revealed to be low-interacting with water molecules. Thus, the reported water models on Au(111)[24] can be treated as the adsorption of water on Au(111) at lower temperatures, while in our case it is difficult for water molecules to be trapped on Au(111) at RT if there is no A molecules.

Note that such rows are the characteristic components of A islands as can be identified from the joint of rows and islands in Fig. 1b and also in Fig. S1 (ESI†). Such a process thus displays the scission of A networks induced by water molecules. Moreover, sequential STM images scanned in the same region display that two rows can wobble around reforming the A island structure *via* inter-row hydrogen bonds (Fig. S2, ESI†), further indicating the dynamic processes between single rows and islands.

Then we expose such a sample to the water atmosphere at a pressure of ~1 × 10^{-5} mbar for 10 min, and small patches of rectangular islands appear with some single rows coexisting (Fig. 1c). Further exposure to the water atmosphere at a higher pressure of ~3 × 10^{-5} mbar for 10 min results in the structural transformation from molecular rows to the rectangular islands (Fig. 1d). Such islands, which are apparently different from the original A islands, tend to grow larger with more and more water. It is worth noting that after water molecules are dosed in the preparation chamber and the sample is transferred to the STM, normally, no further changes in the structures will take place during scanning (from 150 K to RT, except the rare cases of the dynamic processes between single rows and A islands), if no water molecules are further dosed or no further thermal treatments are performed. It is also notable that codeposition of A molecules and water (at the corresponding dosages) results in characteristically the same structures as shown above. On the basis of the above observations together with the previous studies,[17] we assign the rectangular islands to A-H_2O islands, which means water molecules further stitch the A molecular rows by forming new hydrogen bonds.

To gain more structural information of the A-H_2O islands, we have made a detailed comparison between the A-H_2O structures and the original self-assembled A structures (Fig. 2). It is known that A molecules can form both heterochiral and homochiral network structures on Au(111)[22,23] (Fig. 2a and d). The different apparent heights of the A molecules are attributed to herringbone reconstruction, indicating the weak molecule–substrate interactions.[22,23] The corresponding DFT-optimized structural models can be seen in Fig. 2b and e. By systematically analyzing a series of STM images, we also find two kinds of A-H_2O islands with heterochiral or homochiral A molecules involved (Fig. 2c and f) (will be detailed in Fig. 3). Besides, we identify that the A-H_2O structures are constructed by the bright protrusions (highlighted by white circles in Fig. 2c and f) in between, which are distinct from the self-assembled A structures. However, in both heterochiral and homochiral A-H_2O islands, the A molecular rows are the same as the corresponding rows in the self-assembled A islands before hydration. Thus, it implies that water molecules may perturb the initial self-assembled A islands (by selectively breaking the specific hydrogen bonds) and induce them to dissociate into molecular rows in the first step (*i.e.*, scission), and then reform the A-H_2O islands *via* new hydrogen bonds with A molecules (*i.e.*, stitching). In some cases, small patches of A self-assembled structures remain intact and coexist with A-H_2O structures in one island (Fig. S3, ESI†).

Note that such an A-H_2O structure can only be obtained by dosing large amounts of water (at a pressure of ~3 × 10^{-5} mbar for 10 min) at RT. Also, water molecules tend to interact with the polar groups of organic molecules.[16,17,25] Besides, the dimension and topography of one bright protrusion are similar to those of the single water molecule as reported.[5–7,16,17,25] We then attribute each bright protrusion to a water molecule. At the same time, we can observe some blurs at the edges of the islands which may be assigned to the diffusing water molecules.[8] Also note that the canonical form of A is revealed to be the most stable form in the gas phase, in a microhydrated environment and also in the bulk water.[19,20] Thus, we believe that these A-H_2O structures are formed by the canonical A molecules.

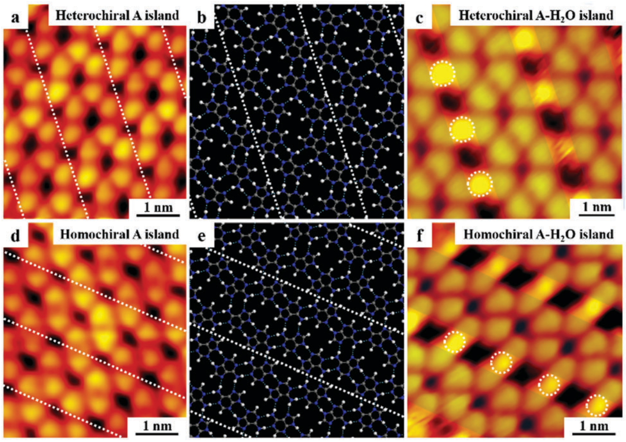

Fig. 2 STM images and DFT-optimized structural models showing the comparisons between self-assembled A islands and the corresponding A-H_2O islands. (a and d) STM images of heterochiral and homochiral self-assembled A islands. (b and e) The corresponding structural models. (c and f) STM images of the corresponding heterochiral and homochiral A-H_2O islands. The white dotted lines in (a), (b), (d) and (e), and highlights in (c) and (f) are depicted to clarify the corresponding molecular rows, respectively.

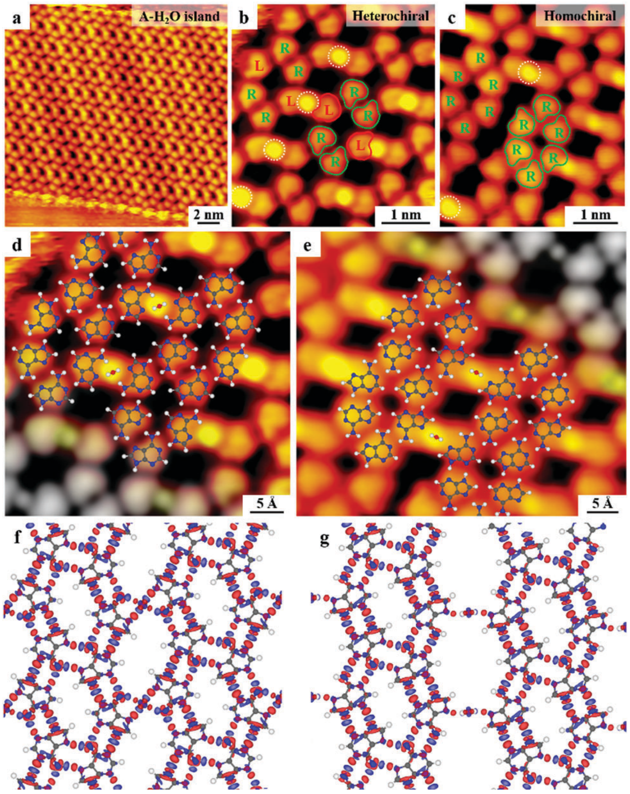

Fig. 3 STM images and DFT-optimized structural models of the A-H_2O islands. (a) Large-scale STM image showing the formation of the A-H_2O island. (b and c) Submolecularly resolved STM images of (b) heterochiral and (c) homochiral A-H_2O islands, respectively, allowing us to identify the molecular chiralities on Au(111) (as indicated by L and R notations and also red and green molecular contours, respectively). The water molecules are indicated by white circles. (d and e) Close-up STM images superimposed with the corresponding DFT-optimized structural models, respectively. The STM simulations (the gray parts) are partially superimposed on the corresponding STM images, respectively. H: white; C: gray; N: blue; and O: red. Scanning conditions: I_t = 0.7 nA, V_t = 2.0 V. (f and g) Charge-density-difference maps of the corresponding structures showing the intermolecular hydrogen bonds at the isosurface value of 0.002 e Å^{-3}. The red and blue isosurfaces indicate charge accumulation and depletion, respectively.

As displayed above (Fig. 1b and Fig. S1, ESI†), the single A molecular rows are always surrounded by the blurs, leading to the difficulty in identifying the chiralities involved. Instead, such chiralities can be identified from the submolecularly resolved STM images (Fig. 3b and c) of the further formed A-H_2O islands. Herein, Fig. 3c is displayed with some vacancy sites (of water) only to make the chiralities of A molecules to be easily identified. An individual A molecule looks similar to a triangle, where the NH_2 group is resolved as a sharp corner. The different chiralities are highlighted by the red and green molecular contours to guide the eye. Based on the STM images, extensive DFT calculations have been performed to reveal the atomic-scale structures. The DFT-optimized structural models together with STM simulations are partially superimposed on the corresponding STM images with good agreements, respectively (Fig. 3d and e). From the structural models and charge-density-difference maps (Fig. 3f and g), we can identify that in the heterochiral structure, water molecules interact with the neighboring A molecules *via* double NH···O and OH···N hydrogen bonds, while in the homochiral one, only double OH···N hydrogen bonds are formed. It is also noticeable that the water molecules are shown as bright protrusions in both A-H_2O structures, which are related to their configurations above the A molecular plane (O atoms are positioned at the highest point). This can also be confirmed from the line profiles (Fig. S4, ESI†). The periodicity of the two networks is slightly different (Fig. S5, ESI†) in accordance with the experimental results (Fig. 3b–e). Despite the weak interactions between Au(111) and water molecules as discussed above, we have also optimized one of the A-H_2O structures including the substrate to explain the situation on Au(111) (Fig. S6, ESI†), where the configuration is similar to that in the gas phase demonstrating the little influence of the substrate.

Moreover, the total binding energies between A rows and water molecules within the A-H_2O islands (0.66 eV and 0.37 eV per unit cell for the heterochiral and homochiral ones, respectively) are calculated to be higher than those between neighboring two A rows within the initial self-assembled A islands (0.40 eV and 0.32 eV per unit cell for heterochiral and homochiral A islands, respectively). This means that the newly formed hydrogen bonds with the involvement of water molecules are more stable than the initial ones, leading to the evolution to the A-H_2O islands. More importantly, according to the systematic theoretical calculations on 21 possible planar A dimers in the gas phase involving the energetics, geometry and electron density as reported,[26] the perturbed A–A binding site in this system (also refer to Fig. 2b and e) is exactly the one with the lowest stabilization energy within these involved A pairs. Thus, the hydration scenario of A networks is speculated to be that (1) at lower water dosages ($\sim 1 \times 10^{-6}$ mbar for 10 min) water molecules first perturb the initial A islands (at the weakest hydrogen bonding sites) by forming stronger hydrogen bonds with A molecules, resulting in the scission of islands into rows (the water molecules may diffuse along the

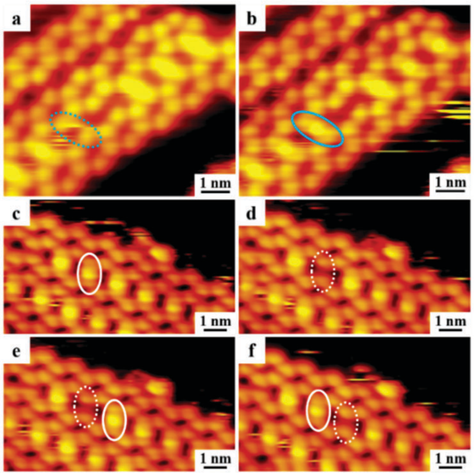

Fig. 4 (a and b) Sequential STM images showing the spontaneous mobility of the water molecule. (c)–(f) Lateral STM manipulations demonstrating the mobility of the water molecules in the island. Scanning conditions: I_t = 0.9 nA, V_t = −1.7 V. The ellipses highlight the target water molecules.

edges of A rows due to the one-sided interactions between water molecules and A rows, which failed to stabilize or trap the water molecules) and (2) then at higher dosages ($\sim 3 \times 10^{-5}$ mbar for 10 min) such neighboring A rows are stitched together by water molecules *via* two-sided hydrogen bonds forming A-H_2O islands and water molecules are also trapped.

Interestingly, sometimes it can be observed that the water molecule trapped in the A-H_2O island may spontaneously diffuse to the vacancy sites (*i.e.*, without binding water molecules) during scanning (Fig. 4a and b). Note that such a situation can only take place when there are vacancy sites in the islands. Inspired by this, we also tried to explore the feasibility of disturbing the water molecules in the A-H_2O island *via* STM manipulations. Using such a strategy, we succeeded in removing the water molecule away from the island (Fig. 4c and d) or moving it to the neighboring vacancy site (Fig. 4e and f). Based on these (Fig. 4), it is further confirmed that the bright protrusion should be attributed to one water molecule as it always moves as a whole entity. Thus, we have successfully achieved the dynamic hydration of self-assembled A structures by the regulation of the amount of water and also by the controlled removal of single water molecules.

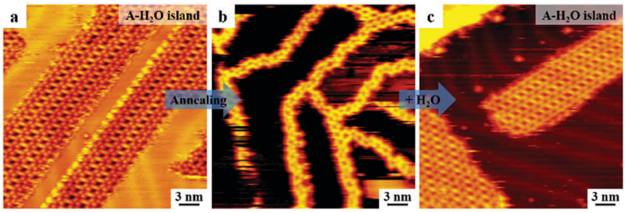

Fig. 5 STM images showing the interconversions between the A-H_2O islands and isolated A rows. (a and b) Structural conversion from A-H_2O islands to A rows by annealing the sample at 350 K. (b and c) Reformation of A-H_2O islands by exposing the sample to the water atmosphere ($\sim 3 \times 10^{-5}$ mbar for 10 min). Scanning conditions: I_t = 1.0 nA, V_t = −1.7 V.

Since we are able to manipulate single water molecules, in the next step, we explore the feasibility of removing more water molecules in the A-H_2O structure. Then we try to anneal the sample (precovered with A-H_2O islands) at 350 K, and obtain the formation of isolated A rows (Fig. 5a and b). Further exposing such a sample to the water atmosphere ($\sim 3 \times 10^{-5}$ mbar for 10 min) leads to the reformation of the A-H_2O islands (Fig. 5b and c). By the removal and addition of water molecules, continuous interconversion of A-H_2O islands and A rows is successfully achieved.

In conclusion, based on high-resolution STM imaging and DFT calculations, we have achieved the controllable scission and stitching of A structures by water molecules representing the dynamic hydration processes, and the water molecules can be removed precisely *via* STM manipulations and thermal treatments. Such results may shed light on the fundamental understanding of water-dependent or water-driven biological processes and heterogeneous catalysis.

The authors acknowledge financial support from the National Natural Science Foundation of China (21473123 and 21622307).

Conflicts of interest

There are no conflicts to declare.

Notes and references

1 P. A. Thiel and T. E. Madey, *Surf. Sci. Rep.*, 1987, **7**, 211.
2 J. Carrasco, A. Hodgson and A. Michaelides, *Nat. Mater.*, 2012, **11**, 667.
3 K. Morgenstern and J. Nieminen, *Phys. Rev. Lett.*, 2002, **88**, 066102.
4 A. Michaelides and K. Morgenstern, *Nat. Mater.*, 2007, **6**, 597.
5 H. Gawronski, K. Morgenstern and K. H. Rieder, *Eur. Phys. J. D*, 2005, **35**, 349.
6 J. Guo, X. Meng, J. Chen, J. Peng, J. Sheng, X. Z. Li, L. Xu, J. R. Shi, E. Wang and Y. Jiang, *Nat. Mater.*, 2014, **13**, 184.
7 J. Chen, J. Guo, X. Meng, J. Peng, J. Sheng, L. Xu, Y. Jiang, X. Z. Li and E. G. Wang, *Nat. Commun.*, 2014, **5**, 4056.
8 A. Shiotari and Y. Sugimoto, *Nat. Commun.*, 2017, **8**, 14313.
9 J. Carrasco, A. Michaelides, M. Forster, S. Haq, R. Raval and A. Hodgson, *Nat. Mater.*, 2009, **8**, 427.
10 Y. He, A. Tilocca, O. Dulub, A. Selloni and U. Diebold, *Nat. Mater.*, 2009, **8**, 585.
11 S. Nie, P. J. Feibelman, N. C. Bartelt and K. Thürmer, *Phys. Rev. Lett.*, 2010, **105**, 026102.
12 T. Yamada, S. Tamamori, H. Okuyama and T. Aruga, *Phys. Rev. Lett.*, 2006, **96**, 036105.
13 J. Cerdá, A. Michaelides, M.-L. Bocquet, P. J. Feibelman, T. Mitsui, M. Rose, E. Fomin and M. Salmeron, *Phys. Rev. Lett.*, 2004, **93**, 116101.
14 S. Maier, B. A. Lechner, G. A. Somorjai and M. Salmeron, *J. Am. Chem. Soc.*, 2016, **138**, 3145.
15 T. Mitsui, M. K. Rose, E. Fomin, D. F. Ogletree and M. Salmeron, *Science*, 2002, **297**, 1850.
16 J. Henzl, K. Boom and K. Morgenstern, *J. Am. Chem. Soc.*, 2014, **136**, 13341.
17 J. Henzl, K. Boom and K. Morgenstern, *J. Chem. Phys.*, 2015, **142**, 101920.
18 C. Zhang, L. Xie, Y. Ding, Q. Sun and W. Xu, *ACS Nano*, 2016, **10**, 3776.
19 J. Gu and J. Leszczynski, *J. Phys. Chem. A*, 1999, **103**, 2744.
20 M. Hanus, M. Kabeláč, J. Rejnek, F. Ryjáček and P. Hobza, *J. Phys. Chem. B*, 2004, **108**, 2087.
21 W. Saenger, *Principles of Nucleic Acid Structure*, Springer-Verlag, New York, 1984, pp. 368–384.
22 R. E. A. Kelly, W. Xu, M. Lukas, R. Otero, M. Mura, Y. J. Lee, E. Lægsgaard, I. Stensgaard, L. N. Kantorovich and F. Besenbacher, *Small*, 2008, **4**, 1494.
23 M. Lukas, R. E. A. Kelly, L. N. Kantorovich, R. Otero, W. Xu, E. Laegsgaard, I. Stensgaard and F. Besenbacher, *J. Chem. Phys.*, 2009, **130**, 024705.
24 D. Stacchiola, J. B. Park, P. Liu, S. Ma, F. Yang, D. E. Starr, E. Muller, P. Sutter and J. Hrbek, *J. Phys. Chem. C*, 2009, **113**, 15102.
25 K. Lucht, D. Loose, M. Ruschmeier, V. Strotkötter, G. Dyker and K. Morgenstern, *Angew. Chem., Int. Ed.*, 2018, DOI: 10.1002/anie.201711062.
26 R. E. A. Kelly, Y. J. Lee and L. N. Kantorovich, *J. Phys. Chem. B*, 2005, **109**, 11933.